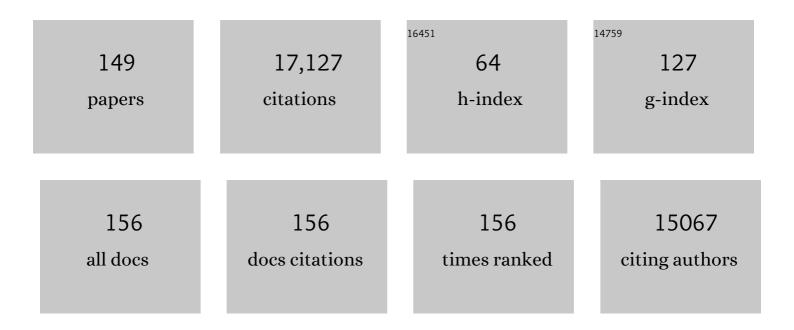
List of Publications by Year in descending order

Source: https://exaly.com/author-pdf/5332769/publications.pdf Version: 2024-02-01



VA-EELLI

#	Article	IF	CITATIONS
1	Single Ir atom anchored in pyrrolic-N4 doped graphene as a promising bifunctional electrocatalyst for the ORR/OER: a computational study. Journal of Colloid and Interface Science, 2022, 607, 1005-1013.	9.4	78
2	Tailoring Competitive Adsorption Sites by Oxygenâ€Vacancy on Cobalt Oxides to Enhance the Electrooxidation of Biomass. Advanced Materials, 2022, 34, e2107185.	21.0	162
3	Dopingâ€Modulated Strain Enhancing the Phosphate Tolerance on PtFe Alloys for Highâ€Temperature Proton Exchange Membrane Fuel Cells. Advanced Functional Materials, 2022, 32, .	14.9	45
4	Artificial Neuron Networks Enabled Identification and Characterizations of 2D Materials and van der Waals Heterostructures. ACS Nano, 2022, 16, 2721-2729.	14.6	22
5	Transforming Electrocatalytic Biomass Upgrading and Hydrogen Production from Electricity Input to Electricity Output. Angewandte Chemie, 2022, 134, .	2.0	17
6	Strain-Assisted Single Pt Sites on High-Curvature MoS ₂ Surface for Ultrasensitive H ₂ S Sensing. CCS Chemistry, 2022, 4, 3842-3851.	7.8	13
7	Laser-assisted high-performance PtRu alloy for pH-universal hydrogen evolution. Energy and Environmental Science, 2022, 15, 102-108.	30.8	66
8	Single Co Sites in Ordered SiO ₂ Channels for Boosting Nonoxidative Propane Dehydrogenation. ACS Catalysis, 2022, 12, 2632-2638.	11.2	52
9	Combined anodic and cathodic hydrogen production from aldehyde oxidation and hydrogen evolution reaction. Nature Catalysis, 2022, 5, 66-73.	34.4	276
10	Pentagonal PdX2 (X = S, Se) nanosheets with X vacancies as high-performance electrocatalysts for the hydrogen evolution reaction. Physical Chemistry Chemical Physics, 2022, , .	2.8	2
11	Activity Origin of Antimony Nanosheets toward Selective Electroreduction of CO ₂ to Formic Acid. Journal of Physical Chemistry C, 2022, 126, 4015-4023.	3.1	7
12	Nano-H-ZSM-5 with Short <i>b</i> -Axis Channels as a Highly Efficient Catalyst for the Synthesis of Ethyl Levulinate from Furfuryl Alcohol. ACS Sustainable Chemistry and Engineering, 2022, 10, 3808-3816.	6.7	5
13	Study on the Structureâ€Activity Relationship Between Singleâ€Atom, Cluster and Nanoparticle Catalysts in a Hierarchical Structure for the Oxygen Reduction Reaction. Small, 2022, 18, e2105487.	10.0	16
14	Lithium Vacancyâ€Tuned [CuO ₄] Sites for Selective CO ₂ Electroreduction to C ₂₊ Products. Small, 2022, 18, e2106433.	10.0	13
15	Active and conductive layer stacked superlattices for highly selective CO2 electroreduction. Nature Communications, 2022, 13, 2039.	12.8	69
16	Why heterogeneous single-atom catalysts preferentially produce CO in the electrochemical CO ₂ reduction reaction. Chemical Science, 2022, 13, 6366-6372.	7.4	35
17	Facet Engineering of Nanoceria for Enzyme-Mimetic Catalysis. ACS Applied Materials & Interfaces, 2022, 14, 21989-21995.	8.0	18
18	High-Performance Ni ₃ P Catalyst for Câ•O Hydrogenation of Ethyl Levulinate: Ni ^{δ+} as Outstanding Adsorption Sites. ACS Catalysis, 2022, 12, 7926-7935.	11.2	13

#	Article	IF	CITATIONS
19	Synthesis of KVPO ₄ F/Carbon Porous Single Crystalline Nanoplates for High-Rate Potassium-Ion Batteries. Nano Letters, 2022, 22, 4933-4940.	9.1	37
20	Fabrication of ternary UiO-66(Ce)/Ag/BiOBr heterojunction for enhanced photocatalytic degradation of ketoprofen via effective electron transfer process: Pathways, DFT calculation and mechanism. Chemosphere, 2022, 305, 135352.	8.2	10
21	2D Multiferroicity with Ferroelectric Switching Induced Spin-Constrained Photoelectricity. ACS Nano, 2022, 16, 11174-11181.	14.6	13
22	Tuning the Selective Adsorption Site of Biomass on Co ₃ O ₄ by Ir Single Atoms for Electrosynthesis. Advanced Materials, 2021, 33, e2007056.	21.0	217
23	Unveiling the Electrooxidation of Urea: Intramolecular Coupling of the Nâ^'N Bond. Angewandte Chemie, 2021, 133, 7373-7383.	2.0	24
24	Unveiling the Electrooxidation of Urea: Intramolecular Coupling of the Nâ^'N Bond. Angewandte Chemie - International Edition, 2021, 60, 7297-7307.	13.8	204
25	Fabrication of Robust Covalent Organic Frameworks for Enhanced Visible-Light-Driven H ₂ Evolution. ACS Catalysis, 2021, 11, 2098-2107.	11.2	116
26	Double sulfur vacancies by lithium tuning enhance CO2 electroreduction to n-propanol. Nature Communications, 2021, 12, 1580.	12.8	162
27	Phase-Controlled Synthesis of Pd–Se Nanocrystals for Phase-Dependent Oxygen Reduction Catalysis. Nano Letters, 2021, 21, 3805-3812.	9.1	46
28	Synergistically electronic tuning of metalloid CdSe nanorods for enhanced electrochemical CO2 reduction. Science China Materials, 2021, 64, 2997-3006.	6.3	20
29	Sn(101) Derived from Metal–Organic Frameworks for Efficient Electrocatalytic Reduction of CO ₂ . Inorganic Chemistry, 2021, 60, 9653-9659.	4.0	24
30	Evolution of dielectric loss-dominated electromagnetic patterns in magnetic absorbers for enhanced microwave absorption performances. Nano Research, 2021, 14, 4006-4013.	10.4	56
31	Electrochemical synthesis of urea on MBenes. Nature Communications, 2021, 12, 4080.	12.8	147
32	Sb ₂ TeSe ₂ Monolayers: Promising 2D Semiconductors for Highly Efficient Excitonic Solar Cells. ACS Omega, 2021, 6, 20590-20597.	3.5	14
33	A Large-Scalable, Surfactant-Free, and Ultrastable Ru-Doped Pt ₃ Co Oxygen Reduction Catalyst. Nano Letters, 2021, 21, 6625-6632.	9.1	43
34	Atomically Precise Dinuclear Site Active toward Electrocatalytic CO ₂ Reduction. Journal of the American Chemical Society, 2021, 143, 11317-11324.	13.7	153
35	NiTe Monolayer: Two-Dimensional Metal with Superior Basal-Plane Activity for the Oxygen Reduction Reaction. Journal of Physical Chemistry C, 2021, 125, 19164-19170.	3.1	12
36	Identification of the hydrogen utilization pathway for the electrocatalytic hydrogenation of phenol. Science China Chemistry, 2021, 64, 1586-1595.	8.2	26

#	Article	IF	CITATIONS
37	Biocompatible Ruthenium Single-Atom Catalyst for Cascade Enzyme-Mimicking Therapy. ACS Applied Materials & Interfaces, 2021, 13, 45269-45278.	8.0	41
38	Double boron atom-doped graphdiynes as efficient metal-free electrocatalysts for nitrogen reduction into ammonia: a first-principles study. Physical Chemistry Chemical Physics, 2021, 23, 17683-17692.	2.8	19
39	Simultaneous diffusion of cation and anion to access N, S co-coordinated Bi-sites for enhanced CO2 electroreduction. Nano Research, 2021, 14, 2790-2796.	10.4	53
40	Simultaneous oxidative and reductive reactions in one system by atomic design. Nature Catalysis, 2021, 4, 134-143.	34.4	132
41	Advances in two dimensional electrochemical catalysts for ammonia synthesis. Chinese Science Bulletin, 2021, 66, 625-639.	0.7	5
42	Deciphering the alternating synergy between interlayer Pt single-atom and NiFe layered double hydroxide for overall water splitting. Energy and Environmental Science, 2021, 14, 6428-6440.	30.8	164
43	Two-Dimensional Biphenylene: A Graphene Allotrope with Superior Activity toward Electrochemical Oxygen Reduction Reaction. Journal of Physical Chemistry Letters, 2021, 12, 12230-12234.	4.6	43
44	Enhanced robustness of half-metallicity in VBr ₃ nanowires by strains and transition metal doping. Physical Chemistry Chemical Physics, 2020, 22, 24455-24461.	2.8	1
45	RuN ₂ Monolayer: A Highly Efficient Electrocatalyst for Oxygen Reduction Reaction. ACS Applied Materials & Interfaces, 2020, 12, 54517-54523.	8.0	22
46	Atomically deviated Pd-Te nanoplates boost methanol-tolerant fuel cells. Science Advances, 2020, 6, eaba9731.	10.3	78
47	Computational Study of Borophene with Line Defects as Sensors for Nitrogen-Containing Gas Molecules. ACS Applied Nano Materials, 2020, 3, 9961-9968.	5.0	24
48	Singleâ€Atom Inâ€Doped Subnanometer Pt Nanowires for Simultaneous Hydrogen Generation and Biomass Upgrading. Advanced Functional Materials, 2020, 30, 2004310.	14.9	77
49	In Situ Topotactic Transformation of an Interstitial Alloy for CO Electroreduction. Advanced Materials, 2020, 32, e2002382.	21.0	56
50	Mesoporous PdAg Nanospheres for Stable Electrochemical CO ₂ Reduction to Formate. Advanced Materials, 2020, 32, e2000992.	21.0	153
51	Coupling N2 and CO2 in H2O to synthesize urea under ambient conditions. Nature Chemistry, 2020, 12, 717-724.	13.6	485
52	Cation Exchange Strategy to Single-Atom Noble-Metal Doped CuO Nanowire Arrays with Ultralow Overpotential for H ₂ O Splitting. Nano Letters, 2020, 20, 5482-5489.	9.1	93
53	Electroactive Metal–Organic Frameworks as Emitters for Selfâ€Enhanced Electrochemiluminescence in Aqueous Medium. Angewandte Chemie - International Edition, 2020, 59, 10446-10450.	13.8	96
54	Optimization of extraction technology of poly-mannuronic acid to a green delivery system for the water-insoluble pesticide, λ-Cyhalothrin. International Journal of Biological Macromolecules, 2020, 153, 17-25.	7.5	5

#	Article	IF	CITATIONS
55	Rational design of dual-metal-site catalysts for electroreduction of carbon dioxide. Journal of Materials Chemistry A, 2020, 8, 15809-15815.	10.3	83
56	Planar Hypercoordinate Motifs in Two-Dimensional Materials. Accounts of Chemical Research, 2020, 53, 887-895.	15.6	54
57	Theoretical screening of single atoms anchored on defective graphene for electrocatalytic N ₂ reduction reactions: a DFT study. Physical Chemistry Chemical Physics, 2020, 22, 9322-9329.	2.8	29
58	Uncovering near-free platinum single-atom dynamics during electrochemical hydrogen evolution reaction. Nature Communications, 2020, 11, 1029.	12.8	379
59	Single-atom catalysts: The role of intrinsic intermediate. Green Energy and Environment, 2020, 5, 4-5.	8.7	14
60	Gadoliniumâ€Induced Valence Structure Engineering for Enhanced Oxygen Electrocatalysis. Advanced Energy Materials, 2020, 10, 1903833.	19.5	114
61	Highly efficient hydrogen production from hydrolysis of ammonia borane over nanostructured Cu@CuCoOx supported on graphene oxide. Journal of Hazardous Materials, 2020, 391, 122199.	12.4	63
62	Engineering Mo/Mo ₂ C/MoC hetero-interfaces for enhanced electrocatalytic nitrogen reduction. Journal of Materials Chemistry A, 2020, 8, 8920-8926.	10.3	54
63	Selective electrochemical production of hydrogen peroxide at zigzag edges of exfoliated molybdenum telluride nanoflakes. National Science Review, 2020, 7, 1360-1366.	9.5	40
64	Two-Dimensional Metal Hexahydroxybenzene Frameworks as Promising Electrocatalysts for an Oxygen Reduction Reaction. ACS Sustainable Chemistry and Engineering, 2020, 8, 7472-7479.	6.7	57
65	In Situ Exfoliation and Pt Deposition of Antimonene for Formic Acid Oxidation via a Predominant Dehydrogenation Pathway. Research, 2020, 2020, 5487237.	5.7	10
66	Enabling Superior Electrochemical Properties for Highly Efficient Potassium Storage by Impregnating Ultrafine Sb Nanocrystals within Nanochannel ontaining Carbon Nanofibers. Angewandte Chemie - International Edition, 2019, 58, 14578-14583.	13.8	332
67	Enabling Superior Electrochemical Properties for Highly Efficient Potassium Storage by Impregnating Ultrafine Sb Nanocrystals within Nanochannel ontaining Carbon Nanofibers. Angewandte Chemie, 2019, 131, 14720-14725.	2.0	53
68	Spin–Orbit Coupling-Dominated Catalytic Activity of Two-Dimensional Bismuth toward CO ₂ Electroreduction: Not the Thinner the Better. Journal of Physical Chemistry Letters, 2019, 10, 4663-4667.	4.6	41
69	Tuning the Electron Localization of Gold Enables the Control of Nitrogenâ€ŧoâ€Ammonia Fixation. Angewandte Chemie - International Edition, 2019, 58, 18604-18609.	13.8	146
70	Tuning the Electron Localization of Gold Enables the Control of Nitrogenâ€ŧoâ€Ammonia Fixation. Angewandte Chemie, 2019, 131, 18777-18782.	2.0	8
71	Highly Active and Selective Electrocatalytic CO ₂ Conversion Enabled by Core/Shell Ag/(Amorphous-Sn(IV)) Nanostructures with Tunable Shell Thickness. ACS Applied Materials & Interfaces, 2019, 11, 39722-39727.	8.0	20
72	A Supported Nickel Catalyst Stabilized by a Surface Digging Effect for Efficient Methane Oxidation. Angewandte Chemie, 2019, 131, 18559-18564.	2.0	20

#	Article	IF	CITATIONS
73	A Supported Nickel Catalyst Stabilized by a Surface Digging Effect for Efficient Methane Oxidation. Angewandte Chemie - International Edition, 2019, 58, 18388-18393.	13.8	69
74	SnP ₂ S ₆ monolayer: a promising 2D semiconductor for photocatalytic water splitting. Physical Chemistry Chemical Physics, 2019, 21, 21064-21069.	2.8	30
75	Unraveling the enzyme-like activity of heterogeneous single atom catalyst. Chemical Communications, 2019, 55, 2285-2288.	4.1	205
76	Boosting Oxygen Reduction Catalysis with Fe–N ₄ Sites Decorated Porous Carbons toward Fuel Cells. ACS Catalysis, 2019, 9, 2158-2163.	11.2	297
77	Structural defects on converted bismuth oxide nanotubes enable highly active electrocatalysis of carbon dioxide reduction. Nature Communications, 2019, 10, 2807.	12.8	456
78	Zirconiumâ€Regulationâ€Induced Bifunctionality in 3D Cobalt–Iron Oxide Nanosheets for Overall Water Splitting. Advanced Materials, 2019, 31, e1901439.	21.0	306
79	Ti ₂ PTe ₂ monolayer: a promising two-dimensional anode material for sodium-ion batteries. RSC Advances, 2019, 9, 15536-15541.	3.6	18
80	Review of twoâ€dimensional materials for electrochemical CO ₂ reduction from a theoretical perspective. Wiley Interdisciplinary Reviews: Computational Molecular Science, 2019, 9, e1416.	14.6	59
81	TMC (TM = Co, Ni, and Cu) monolayers with planar pentacoordinate carbon and their potential applications. Journal of Materials Chemistry C, 2019, 7, 6406-6413.	5.5	29
82	Frontispiz: A Supported Nickel Catalyst Stabilized by a Surface Digging Effect for Efficient Methane Oxidation. Angewandte Chemie, 2019, 131, .	2.0	0
83	Defectsâ€Induced Inâ€Plane Heterophase in Cobalt Oxide Nanosheets for Oxygen Evolution Reaction. Small, 2019, 15, e1904903.	10.0	69
84	Activity Origin and Design Principles for Oxygen Reduction on Dual-Metal-Site Catalysts: A Combined Density Functional Theory and Machine Learning Study. Journal of Physical Chemistry Letters, 2019, 10, 7760-7766.	4.6	149
85	Frontispiece: A Supported Nickel Catalyst Stabilized by a Surface Digging Effect for Efficient Methane Oxidation. Angewandte Chemie - International Edition, 2019, 58, .	13.8	1
86	Two-dimensional transition metal diborides: promising Dirac electrocatalysts with large reaction regions toward efficient N ₂ fixation. Journal of Materials Chemistry A, 2019, 7, 25887-25893.	10.3	45
87	Bridging the Surface Charge and Catalytic Activity of a Defective Carbon Electrocatalyst. Angewandte Chemie - International Edition, 2019, 58, 1019-1024.	13.8	224
88	BN Pairs Enriched Defective Carbon Nanosheets for Ammonia Synthesis with High Efficiency. Small, 2019, 15, e1805029.	10.0	164
89	Catalytic Hydrogenation of Nitrophenols by Cubic and Hexagonal Phase Unsupported Ni Nanocrystals. ChemistrySelect, 2019, 4, 42-48.	1.5	10
90	Photoelectrochemical Synthesis of Ammonia on the Aerophilic-Hydrophilic Heterostructure with 37.8% Efficiency. CheM, 2019, 5, 617-633.	11.7	241

#	Article	IF	CITATIONS
91	Solid-Diffusion Synthesis of Single-Atom Catalysts Directly from Bulk Metal for Efficient CO2 Reduction. Joule, 2019, 3, 584-594.	24.0	277
92	Bridging the Surface Charge and Catalytic Activity of a Defective Carbon Electrocatalyst. Angewandte Chemie, 2019, 131, 1031-1036.	2.0	41
93	Exploring the Performance Improvement of the Oxygen Evolution Reaction in a Stable Bimetal–Organic Framework System. Angewandte Chemie, 2018, 130, 9808-9812.	2.0	54
94	Exploring the Performance Improvement of the Oxygen Evolution Reaction in a Stable Bimetal–Organic Framework System. Angewandte Chemie - International Edition, 2018, 57, 9660-9664.	13.8	340
95	Tuning Surface Electronic Configuration of NiFe LDHs Nanosheets by Introducing Cation Vacancies (Fe or Ni) as Highly Efficient Electrocatalysts for Oxygen Evolution Reaction. Small, 2018, 14, e1800136.	10.0	341
96	Ultrathin bismuth nanosheets from in situ topotactic transformation for selective electrocatalytic CO2 reduction to formate. Nature Communications, 2018, 9, 1320.	12.8	658
97	The germanium telluride monolayer: a two dimensional semiconductor with high carrier mobility for photocatalytic water splitting. Journal of Materials Chemistry A, 2018, 6, 4119-4125.	10.3	87
98	Ru Modulation Effects in the Synthesis of Unique Rod-like Ni@Ni ₂ P–Ru Heterostructures and Their Remarkable Electrocatalytic Hydrogen Evolution Performance. Journal of the American Chemical Society, 2018, 140, 2731-2734.	13.7	326
99	Enhancement of Schizochytrium DHA synthesis by plasma mutagenesis aided with malonic acid and zeocin screening. Applied Microbiology and Biotechnology, 2018, 102, 2351-2361.	3.6	43
100	Single Pt Atoms Confined into a Metal–Organic Framework for Efficient Photocatalysis. Advanced Materials, 2018, 30, 1705112.	21.0	599
101	Pd ₂ Se ₃ monolayer: a novel two-dimensional material with excellent electronic, transport, and optical properties. Journal of Materials Chemistry C, 2018, 6, 4494-4500.	5.5	36
102	Low Overpotential for Electrochemically Reducing CO ₂ to CO on Nitrogen-Doped Graphene Quantum Dots-Wrapped Single-Crystalline Gold Nanoparticles. ACS Energy Letters, 2018, 3, 946-951.	17.4	48
103	Tuning the activity of the inert MoS ₂ surface <i>via</i> graphene oxide support doping towards chemical functionalization and hydrogen evolution: a density functional study. Physical Chemistry Chemical Physics, 2018, 20, 1861-1871.	2.8	22
104	Histone acetylation of oligodendrocytes protects against white matter injury induced by inflammation and hypoxia-ischemia through activation of BDNF-TrkB signaling pathway in neonatal rats. Brain Research, 2018, 1688, 33-46.	2.2	15
105	Synergistic effect of well-defined dual sites boosting the oxygen reduction reaction. Energy and Environmental Science, 2018, 11, 3375-3379.	30.8	528
106	Phase and structure engineering of copper tin heterostructures for efficient electrochemical carbon dioxide reduction. Nature Communications, 2018, 9, 4933.	12.8	141
107	PtTe Monolayer: Two-Dimensional Electrocatalyst with High Basal Plane Activity toward Oxygen Reduction Reaction. Journal of the American Chemical Society, 2018, 140, 12732-12735.	13.7	95
108	Insights into Hydrotropic Solubilization for Hybrid Ion Redox Flow Batteries. ACS Energy Letters, 2018, 3, 2641-2648.	17.4	54

#	Article	IF	CITATIONS
109	Selective CO ₂ Reduction on 2D Mesoporous Bi Nanosheets. Advanced Energy Materials, 2018, 8, 1801536.	19.5	274
110	Encapsulation of Ni ₃ Fe Nanoparticles in Nâ€Doped Carbon Nanotube–Grafted Carbon Nanofibers as Highâ€Efficiency Hydrogen Evolution Electrocatalysts. Advanced Functional Materials, 2018, 28, 1805828.	14.9	168
111	Stabilizing and Activating Metastable Nickel Nanocrystals for Highly Efficient Hydrogen Evolution Electrocatalysis. ACS Nano, 2018, 12, 11625-11631.	14.6	55
112	PdSeO ₃ Monolayer: Promising Inorganic 2D Photocatalyst for Direct Overall Water Splitting Without Using Sacrificial Reagents and Cocatalysts. Journal of the American Chemical Society, 2018, 140, 12256-12262.	13.7	216
113	Global minimum beryllium hydride sheet with novel negative Poisson's ratio: first-principles calculations. RSC Advances, 2018, 8, 19432-19436.	3.6	7
114	Innentitelbild: Exploring the Performance Improvement of the Oxygen Evolution Reaction in a Stable Bimetal-Organic Framework System (Angew. Chem. 31/2018). Angewandte Chemie, 2018, 130, 9702-9702.	2.0	0
115	Preferential Cation Vacancies in Perovskite Hydroxide for the Oxygen Evolution Reaction. Angewandte Chemie, 2018, 130, 8827-8832.	2.0	37
116	Preferential Cation Vacancies in Perovskite Hydroxide for the Oxygen Evolution Reaction. Angewandte Chemie - International Edition, 2018, 57, 8691-8696.	13.8	337
117	Atomically dispersed Au1 catalyst towards efficient electrochemical synthesis of ammonia. Science Bulletin, 2018, 63, 1246-1253.	9.0	225
118	Facile synthesis of highly monodisperse EuSe nanocubes with size-dependent optical/magnetic properties and their electrochemiluminescence performance. Nanoscale, 2018, 10, 13617-13625.	5.6	9
119	Two-Dimensional C ₄ N Global Minima: Unique Structural Topologies and Nanoelectronic Properties. Journal of Physical Chemistry C, 2017, 121, 2669-2674.	3.1	49
120	GeP ₃ : A Small Indirect Band Gap 2D Crystal with High Carrier Mobility and Strong Interlayer Quantum Confinement. Nano Letters, 2017, 17, 1833-1838.	9.1	338
121	CoV ₂ O ₆ –V ₂ O ₅ Coupled with Porous N-Doped Reduced Graphene Oxide Composite as a Highly Efficient Electrocatalyst for Oxygen Evolution. ACS Energy Letters, 2017, 2, 1327-1333.	17.4	84
122	Theoretical and experimental studies on three water-stable, isostructural, paddlewheel based semiconducting metal–organic frameworks. Dalton Transactions, 2017, 46, 8204-8218.	3.3	20
123	Dirac Nodal Lines and Tilted Semi-Dirac Cones Coexisting in a Striped Boron Sheet. Journal of Physical Chemistry Letters, 2017, 8, 1707-1713.	4.6	81
124	Rapid exfoliation of layered covalent triazine-based frameworks into N-doped quantum dots for the selective detection of Hg ²⁺ ions. Journal of Materials Chemistry A, 2017, 5, 9272-9278.	10.3	76
125	Role of HMGB1 translocation to neuronal nucleus in rat model with septic brain injury. Neuroscience Letters, 2017, 645, 90-96.	2.1	5
126	Benzene-like N ₆ rings in a Be ₂ N ₆ monolayer: a stable 2D semiconductor with high carrier mobility. Journal of Materials Chemistry C, 2017, 5, 11515-11521.	5.5	15

#	Article	IF	CITATIONS
127	Filling the oxygen vacancies in Co ₃ O ₄ with phosphorus: an ultra-efficient electrocatalyst for overall water splitting. Energy and Environmental Science, 2017, 10, 2563-2569.	30.8	859
128	Effective Interlayer Engineering of Two-Dimensional VOPO ₄ Nanosheets via Controlled Organic Intercalation for Improving Alkali Ion Storage. Nano Letters, 2017, 17, 6273-6279.	9.1	102
129	Significantly Enhanced Hydrogen Evolution Activity of Freestanding Pdâ€Ru Distorted Icosahedral Clusters with less than 600 Atoms. Chemistry - A European Journal, 2017, 23, 18203-18207.	3.3	24
130	Cesium Lead Halide Perovskite Quantum Dots as a Photoluminescence Probe for Metal Ions. Advanced Materials, 2017, 29, 1700150.	21.0	112
131	Ultrathin Layers of PdPX (X=S, Se): Two Dimensional Semiconductors for Photocatalytic Water Splitting. Chemistry - A European Journal, 2017, 23, 13612-13616.	3.3	66
132	FeB ₆ Monolayers: The Graphene-like Material with Hypercoordinate Transition Metal. Journal of the American Chemical Society, 2016, 138, 5644-5651.	13.7	219
133	Band-gap modulation of C4H nanosheets by interlayer weak interaction and external electric field: a computational study. Theoretical Chemistry Accounts, 2016, 135, 1.	1.4	2
134	Two-dimensional nanostructures of non-layered ternary thiospinels and their bifunctional electrocatalytic properties for oxygen reduction and evolution: the case of CuCo ₂ S ₄ nanosheets. Inorganic Chemistry Frontiers, 2016, 3, 1501-1509.	6.0	69
135	Dirac State in the FeB ₂ Monolayer with Graphene-Like Boron Sheet. Nano Letters, 2016, 16, 6124-6129.	9.1	200
136	Ultrasmall and phase-pure W2C nanoparticles for efficient electrocatalytic and photoelectrochemical hydrogen evolution. Nature Communications, 2016, 7, 13216.	12.8	334
137	Semi-metallic Be5C2 monolayer global minimum with quasi-planar pentacoordinate carbons and negative Poisson's ratio. Nature Communications, 2016, 7, 11488.	12.8	247
138	Semiconducting Groupâ€15 Monolayers: A Broad Range of Band Gaps and High Carrier Mobilities. Angewandte Chemie - International Edition, 2016, 55, 1666-1669.	13.8	651
139	Germanium monosulfide monolayer: a novel two-dimensional semiconductor with a high carrier mobility. Journal of Materials Chemistry C, 2016, 4, 2155-2159.	5.5	212
140	Monoclinic Copper(I) Selenide Nanocrystals and Copper(I) Selenide/Palladium Heterostructures: Synthesis, Characterization, and Surface-Enhanced Raman Scattering Performance. European Journal of Inorganic Chemistry, 2015, 2015, 2229-2236.	2.0	13
141	Band gap modulation of Janus graphene nanosheets by interlayer hydrogen bonding and the external electric field: a computational study. Journal of Materials Chemistry C, 2015, 3, 3416-3421.	5.5	50
142	Synthesis and evaluation of novel N-3-benzimidazolephenylbisamide derivatives for antiproliferative and Hedgehog pathway inhibitory activity. MedChemComm, 2015, 6, 1137-1142.	3.4	6
143	Not your familiar two dimensional transition metal disulfide: structural and electronic properties of the PdS ₂ monolayer. Journal of Materials Chemistry C, 2015, 3, 9603-9608.	5.5	135
144	Fluorine-Doped Carbon Particles Derived from Lotus Petioles as High-Performance Anode Materials for Sodium-Ion Batteries. Journal of Physical Chemistry C, 2015, 119, 21336-21344.	3.1	158

#	Article	IF	CITATIONS
145	Be ₂ C Monolayer with Quasiâ€Planar Hexacoordinate Carbons: A Global Minimum Structure. Angewandte Chemie - International Edition, 2014, 53, 7248-7252.	13.8	223
146	Preserving the edge magnetism of graphene nanoribbons by iodine termination: a computational study. Theoretical Chemistry Accounts, 2014, 133, 1.	1.4	2
147	Self-Modulated Band Structure Engineering in C ₄ F Nanosheets: First-Principles Insights. Journal of Chemical Theory and Computation, 2014, 10, 1265-1271.	5.3	23
148	Graphene Nanoribbons: An Effective Approach to Achieve a Spin Gapless Semiconductor–Halfâ€Metal–Metal Transition in Zigzag Graphene Nanoribbons: Attaching A Floating Induced Dipole Field via <i>π</i> 〓 <i>π</i> Interactions (Adv. Funct. Mater. 12/2013). Advanced Functional Materials, 2013, 23, 1478-1478.	14.9	1
149	Electronic and Magnetic Properties of BN Monolayer Sheets with H- or O-Saturated Vacancies: A First-Principles Study. Journal of Computational and Theoretical Nanoscience, 2011, 8, 1513-1519.	0.4	10